Chapter 4
Evaluating In Vitro Angiogenesis Using Live Cell Imaging

Elen Bray and Mark Slevin

4.1 Introduction

In today's research laboratories the use of microscopy most commonly involves the manual visualisation and capture of experimental examples at specific time points, normally at the beginning and end of a study. Although informative these approaches are often labour intensive, subjective and run the risk of vital information being missed or misinterpreted, as data from only a fraction of the experimental time period is collected. In addition, information on cellular movement, interactions and behaviour cannot be obtained using such techniques.

The ability to continually monitor and obtain kinetic experimental data has become a desired tool in many research fields, and as a result many microscopes have since added an environmental chamber to their platform, offering a form of live cell kinetic imaging. In practice however, sample throughput and analysis capabilities are often limited on these systems with environmental conditions not remaining optimal for long term experiments.

Recent advances in image acquisition technology and software algorithms have enabled specialised live cell imaging platforms to be developed. One such system is Cell-IQ™, which combines optimised incubation conditions with phase contrast/fluorescence imaging and analysis, allowing long term kinetic cell studies to be performed for extended periods of time.

The additional information that kinetic live cell imaging can provide makes it a suitable and appealing tool for a large number of fields including stem cell research [1–4], oncology [5], neuroscience research [6, 7], drug discovery [8] and angiogenesis [9].

E. Bray (✉)
CM Technologies Oy, Biokatu 12, 33520 Tampere, Finland

M. Slevin
School of Healthcare Science, Manchester Metropolitan University, Manchester, UK

M. Slevin, G. McDowell (eds.), *Handbook of Vascular Biology Techniques*,
DOI 10.1007/978-94-017-9716-0_4

Angiogenesis plays a critical role in the repair, replacement and cellular survival following tissue damage. The in-vitro angiogenic assays commonly used to assess the biological activity of potential pro- or anti-angiogenic therapies include cell migration and tubule formation assays. Traditionally cell migration is measured using a 2D wound healing assay, an in-vitro assay where a scratch is made through the centre of a confluent cellular layer and the rate of healing calculated via changes in wound width measurements and wound area. The formation of tubules is commonly aided by culturing the cells at specific densities on extracellular matrices such as matrigel.

Measurements for both assays traditionally involve the manual capture of images at specific time intervals, followed by manual measurements using basic software tools.

The following chapter aims to discuss how kinetic live cell imaging is an appropriate and valuable tool for studying the in–vitro angiogenic process in real time.

4.2 Methodology

4.2.1 Instrumentation- Cell-IQ®

Cell-IQ® is a fully integrated live cell imaging and analysis platform. The temperature controlled incubator, tailored gaseous environment and the use of light emitting diodes for both phase and fluorescence imaging creates an optimised cellular environment, allowing biological responses to be monitored in real time from a few hours to many weeks.

The incubator is integrated into the system (+/−0.5 °C) and houses two independent controlled gas lines. These gas lines feed directly into the culture vessel through specially designed cell secure™ lids. The gas mix is user defined and as the two lines are independent, different gas mixes can be fed to the two positions, allowing for example normoxic and hypoxic studies to run simultaneously.

Images are captured using a CCD camera, and a high precision motorised stage (XY = +/−1 μM Z = +/−0.4 μM) controls the movement of the culture vessel, allowing images to be acquired from any X, Y, Z position within the plate/dish/slide/flask.

Unlike many traditional microscopes the Cell-IQ® is able to image samples using variable sized Z-stacks (user defined), accommodating both 2D and 3D structures [10]. The final images are generated by creating a unique ‘all-in-focus image’. This is achieved by collating together the best focused pixels from each Z level at every XY position (Diagram 4.1). The generated high quality single image is ideal for data processing [11].

Additional imaging features include ‘auto focus’, a focusing tool which will automatically focus the region of interest for the user and ‘auto-adjust focus’.

Independent to the ‘auto-focus’ the ‘auto-adjust focus’ enables the defined Z-stack to re-adjust its position over time as the cells/structures change position. The benefit of such technology is not only can cells/structures which exist in different planes be focused simultaneously, but they will also remain in focus as their positions move through the different Z planes.

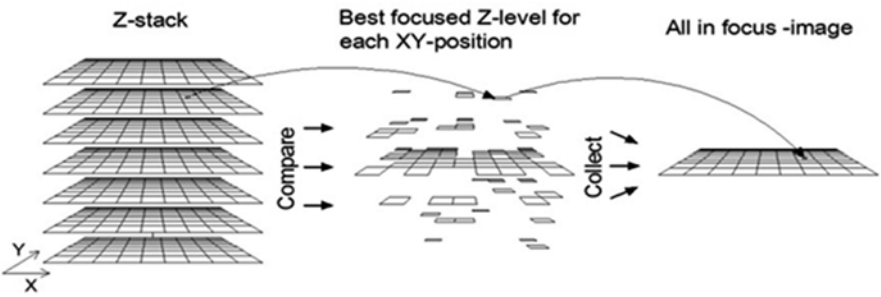

Diagram 4.1 A schematic diagram detailing the generation of an‘ all in focus image’ created by Imagen software

Accompanying the hardware is the Cell-IQ® analyser™ software programme. This software utilises ‘machine vision technology’, pattern recognition software which is traditionally used in medical imaging and precision robotics [12].

This software enables the user to teach the system to recognise different patterns, allowing user defined protocols to be created that distinguish between morphologically different structures, for example different cell types or different phases such as live and dead cells. Once taught this cell counting and classification tool is able to automatically identify and quantify the specified cellular structures in each of the captured images.

Additional tools based on threshold measurements are also provided as separate tools in the software. These tools automatically measure changes in area or wound widths, fluorescence intensity and area, which in conjunction with the machine vision capabilities facilitates all aspects of the in vitro angiogenesis process to be quantified automatically.

4.3 Materials

4.3.1 General

Cell-IQ® Imaging and analysis platform (including appropriate objective)
Cell Secure™ lids
Sterile phosphate buffered saline (PBS)
Pressure Regulator

- Single stage cylinder regulator
- Outlet pressure 0.2–3 bar
- Valve connection DIN 10 and 6 mm (tubing)

Electrical Tape
0.2 μM Filters
Premixed gaseous mixture (e.g. 5 % CO_2 mixed with air)

4.3.2 Scratch Wound

P200 pipette tip
10x objective (CFI Achromat Phase contrast ADL 10x)
24 well plate (standard SBS plate footprint)

4.3.3 Tubule Formation

Growth factor reduced matrigel (BD Biosciences)
10x objective (CFI Achromat Phase contrast ADL 10x)
48 well plate (Standard SBS plate footprint)

4.4 Basic Protocol

4.4.1 Scratch Wound (Mouse Embryo Fibrosarcoma Cells)

Nine wells of a twenty-four well plate were seeded with mouse embryo fibrosarcoma cells (generated from single VEGF isoform expressing mice, specifically the VEGF164 isoform) [13], and incubated at 37 °C/5 % CO_2 until the cells achieved 100 % confluence. The cells were then washed with PBS and an artificial wound created using a commercially available automated wound maker. Prior to imaging, the cells were washed with PBS (Invitrogen) and the media replenished with, (i) fresh culture medium (high glucose DMEM (Invitrogen) medium containing L-glutamine, Fetal Calf Serum (FBS), and the antibiotics G-418 and puromycin), (ii) fresh culture medium plus drug X, (iii) fresh culture medium plus drug Y. Triplicate wells of the treatment were set up.

The plate was subsequently prepared for imaging. In order to prevent media evaporation, PBS was added to all the empty wells to help humidify the flowing gas. The plate was then secured with a cell Secure™ lid and sealed using electrical tape, creating an enclosed environment.

Using the Cell IQ™ Imagen software, two regions of interest (ROI) were selected from each well and imaged automatically every 30 min for a period of 65 h. Images were captured using a Z stack of 20 μM with the 'auto-adjust focus' activated.

Data is presented by the change in wound width over time and by the percentage by which the original scratch wound width has decreased.

The captured images were subsequently analysed using the Analyser™ software scratch wound analysis tool. Using threshold measurements, the tool is able to calculate the closure of the wound automatically over time.

4.4.2 Co-culture Scratch Wound (HaCaT and L929 Cells)

Tissue culture plates (24 well) were collagen-coated by adding 0.2 mg/ml of collagen type I solution (Sigma, Dorset UK) for 2 h at 37 °C before rinsing with PBS (Invitrogen).

Each well was seeded with HaCaT (keratinocyte cells) and L929 (Fibroblasts cells) to give a final density of 100,000 cells per well (equal numbers of each cell type) and maintained at 37 °C and 5 % CO_2 for 24 h to permit cell adhesion and the formation of a confluent monolayer. These confluent monolayers were then scored with a sterile pipette tip to leave a scratch of approximately 0.4–0.5 mm in width. Culture medium was then immediately removed (along with any dislodged cells) and replaced with (i) fresh serum supplemented culture medium (10 % FCS), or (ii) conditioned medium which had been generated from culturing Mesenchymal stem cells under serum free conditions (MSC-CM). Each treatment was performed in quadruplicate [14].

Prior to imaging with Cell-IQ®, the plates were prepared as described above. Pre-selected fields were imaged continually (every 6 min) until wound closure was complete.

Data is presented as the percentage by which the original scratch wound width has decreased for each given time point. In addition, for the duration of the closure, both L929 and HaCaT cell numbers were quantified using the automated cell counting and classification tool to try and establish if both or just one cell type was contributing to the closure of the wound.

4.4.3 Tubule Formation Assay

A pre-chilled 48 well plate was coated with 100 µl of undiluted growth factor reduced matrigel (BD Biosciences) on ice. In order to allow the matrigel to polymerise, the plate was incubated for an hour at 37 °C. Human umbilical vein endothelial cells (HUVECs) were seeded at a density of 4×10^4cells/well and the plate prepared for live cell imaging as previously described.

In order to monitor larger areas, a large field of view can be generated by adding a number of positions as a grid and stitching them into a single image. For this experiment a 3×3 grid was added and the cells were imaged every 30 min for a period of 22 h. In order to ensure the three dimensional tubule structures remained in focus over time a 50 µM Z-stack with the 'auto-adjust feature' activated was applied in the imaging settings.

Images were subsequently analysed using the tubule and branch-point Analyser™ tool, and the data is presented as total tubule length and the total number of different branch points over time.

4.5 Results

4.5.1 Scratch Wound (Mouse Embryo Fibrosarcoma Cells)

The data generated clearly illustrates that both treatments (drug X and Y) enhance wound healing, accelerating the rate of closure (Figs. 4.3 and 4.4). The automated results allow closure times to be easily and accurately identified, allowing the exact difference between the rates of closure for different treatment groups to be documented.

4.5.2 Wound Closure: Co-culture (HaCaT and L929 Cells)

Below are sample results showing scratch wound closure assay at increasing time points culminating in complete resolution.

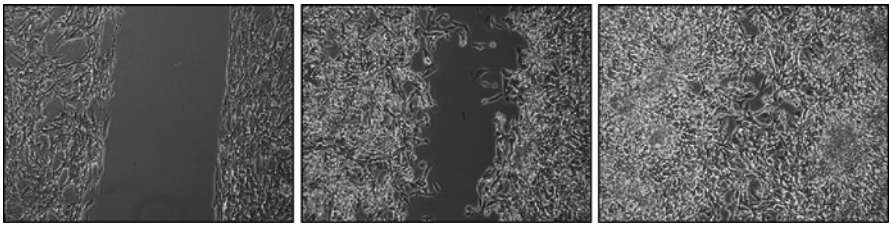

Fig. 4.1 Example of the captured scratch wound using the Cell-IQ Imagen acquisition software

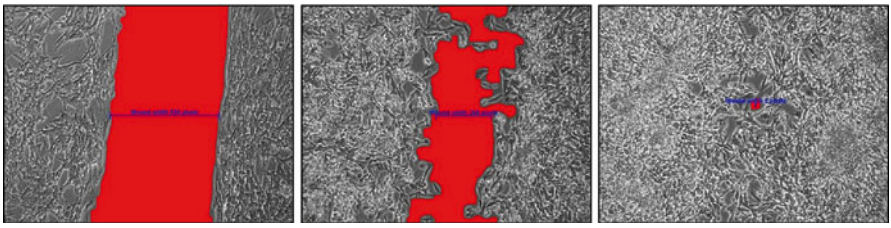

Fig. 4.2 Example of the analysed scratch wound using Analyser software

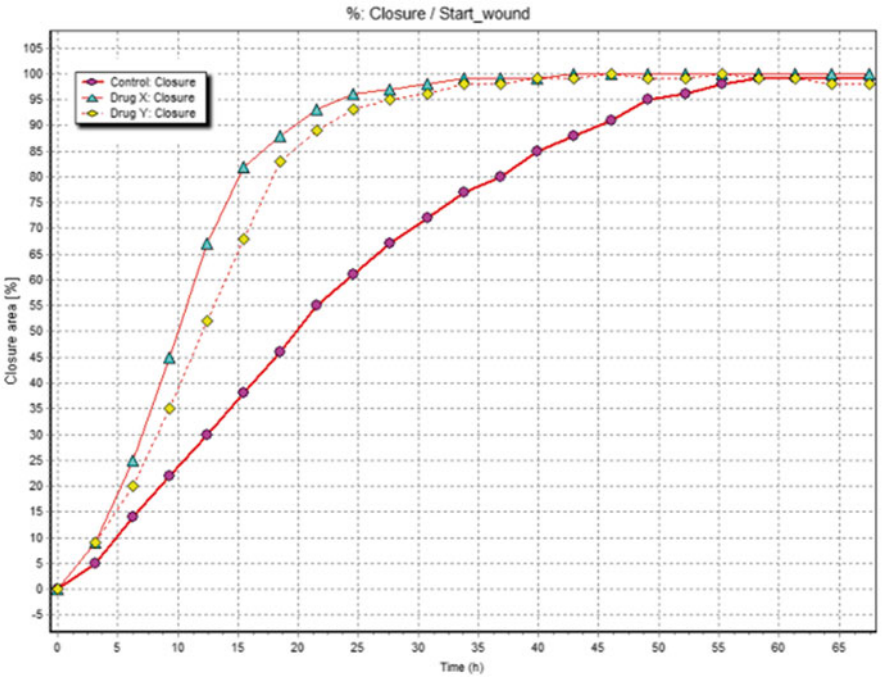

Fig. 4.3 Graphical results illustrating the percentage closure of the scratch wounds over time (Data obtained from two positions in three replicate wells ($n=6$))

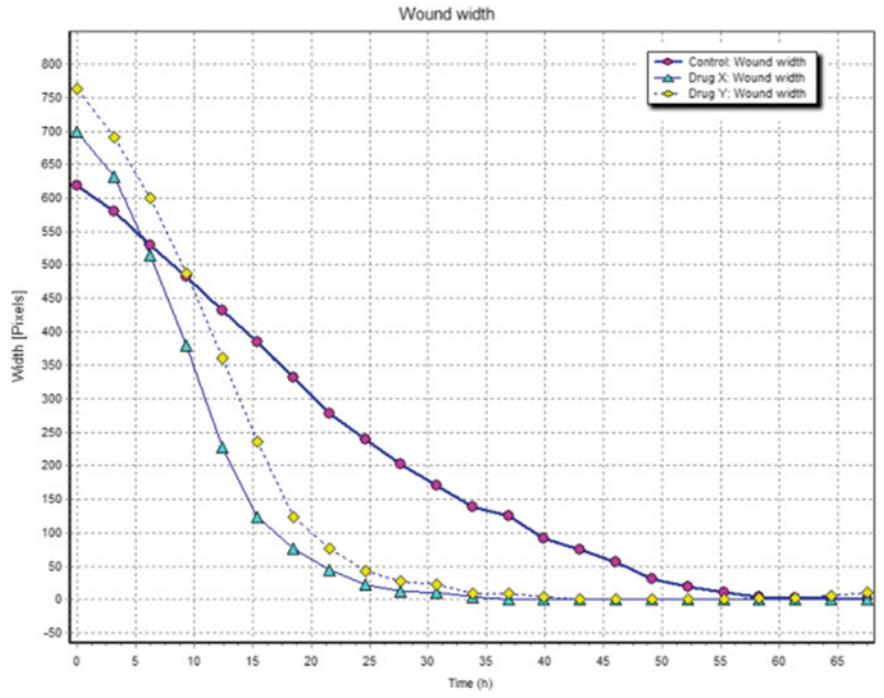

Fig. 4.4 Graphical results illustrating the change in wound width over time (Data obtained from two positions in three replicate wells ($n=6$))

4.5.3 Co-culture Analysis-Cell Classification

In order to distinguish between different cell types/phases using the analyser software a sample library needs to be created (Fig. 4.7). This is achieved through selecting examples of each of the different phases/cell types and using these as representatives to generate a protocol.

In order to determine if a single cell type was contributing to the closure of the co-culture scratch wound, a sample library was created categorising L929 cells (fibroblasts) and HaCaT cells (keratinocytes). The protocol generated was then used to quantify the number of each cell type in each captured image over the 96 h time period.

4.5.3.1 Cell Sample Library

The generated results illustrated that the MSC-CM enhanced the rate of the scratch wound closure, accelerating the closure time by approx. 30 h (Figs. 4.5 and 4.6).

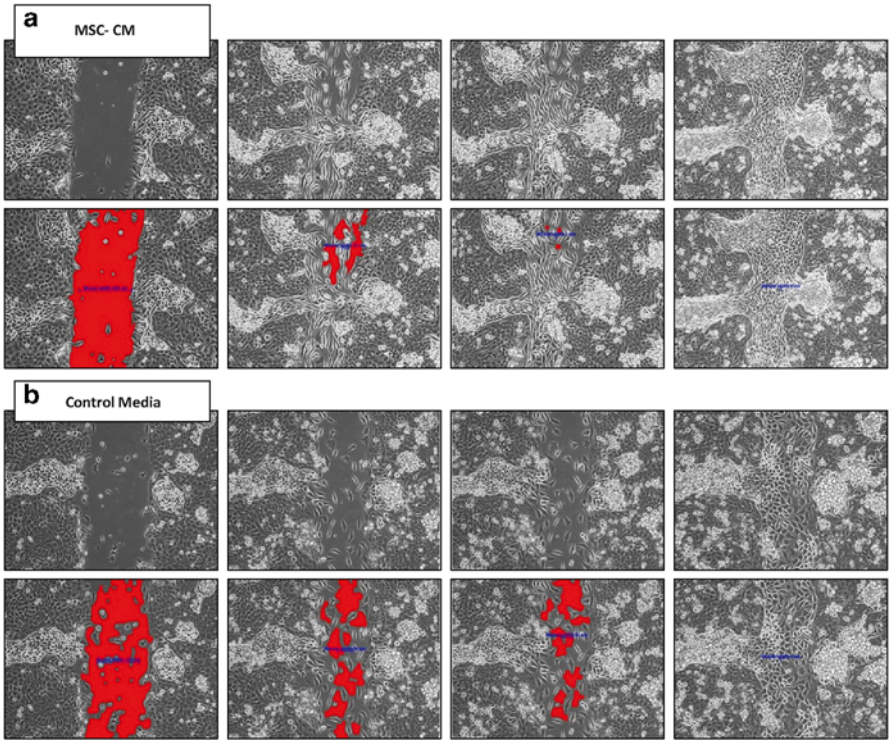

Fig. 4.5 Example of the captured and corresponding analysed scratch wound images over 96 h using (**a**) conditioned MSC media (**b**) control media

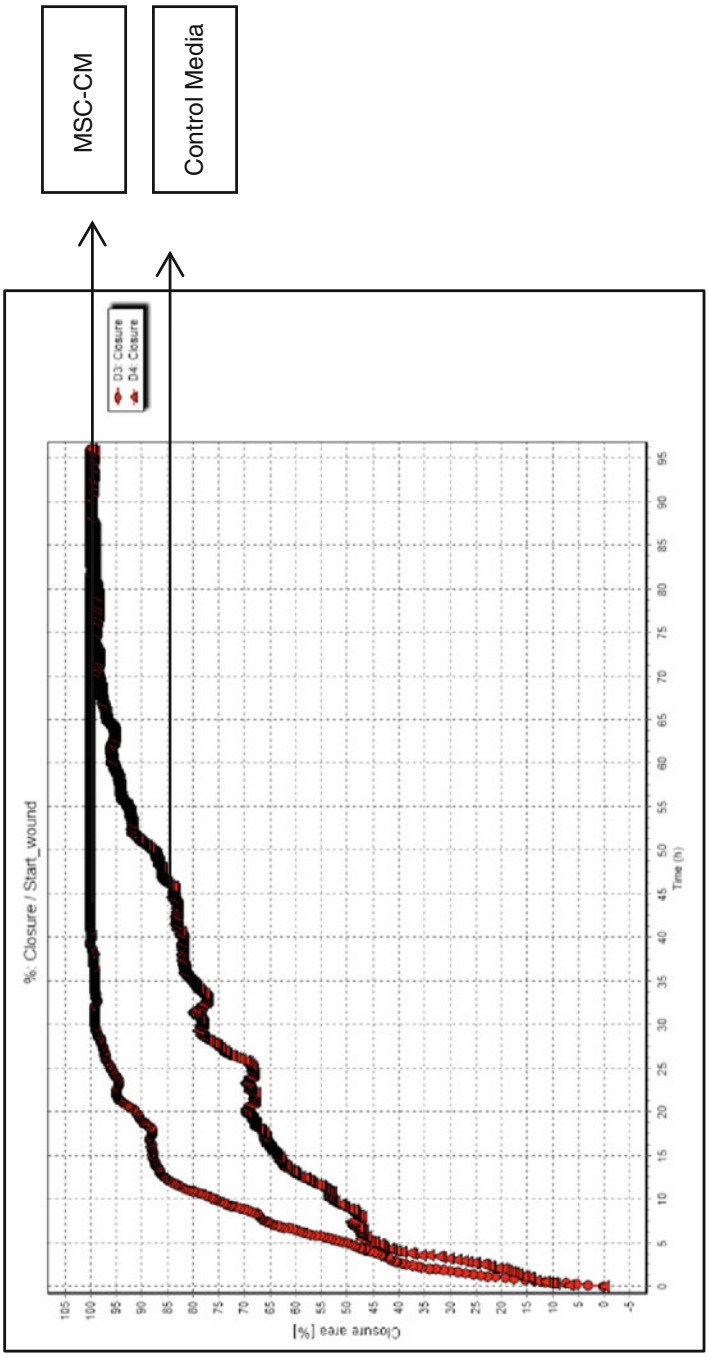

Fig. 4.6 Graphical results illustrating the percentage closure of the scratch wounds over a 96 h time period

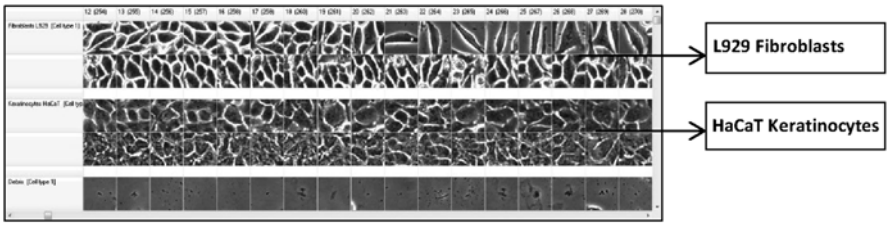

Fig. 4.7 A snapshot of the sample library used to generate the protocol to distinguish between L929 and HaCaT cells

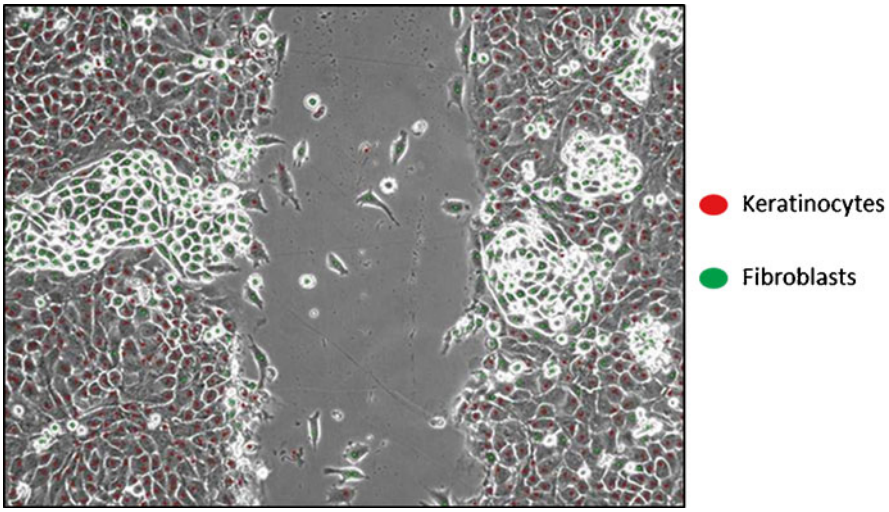

Fig. 4.8 Analysed image demonstrating the identification of the different cell types in the absence of any fluorescent labelling. The *red dots* indicate the identification of HaCaT keratinocyte cells, and the *green dots* represent the L929 fibroblast cells

The quantification of the different cell types revealed an increase in the number of L929 fibroblast cells during the closure of the wound, suggesting that it was the L929 fibroblast cells that migrated into the wound, facilitating its closure. This result is seen irrespective of the media used (Fig. 4.9).

The above detailed classification results were subsequently verified by fluorescent data.

Both cell types were fluorescently labelled and a snapshot of their location over the 96 h obtained through manual imaging [12].

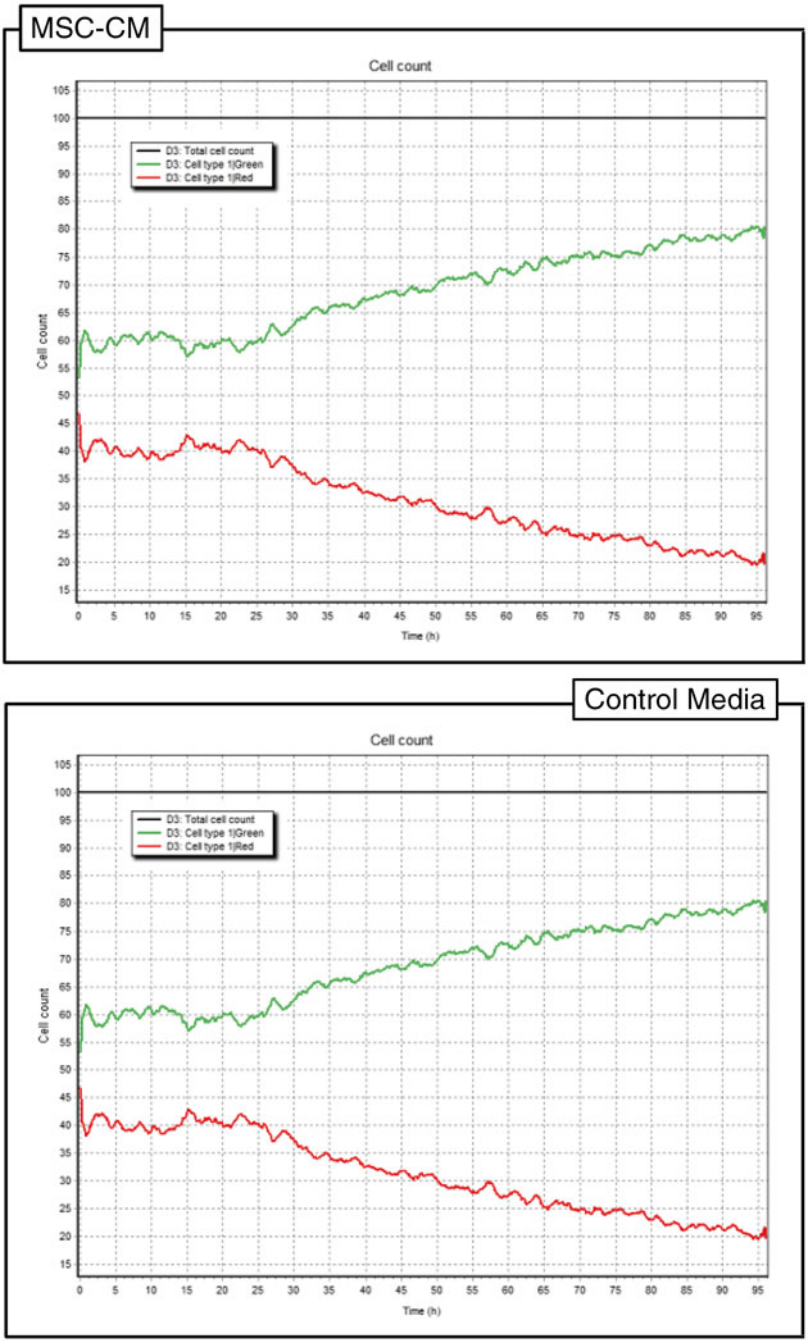

Fig. 4.9 Quantification data demonstrating the percentage of each cell type identified during the closure of the wound over 96 h

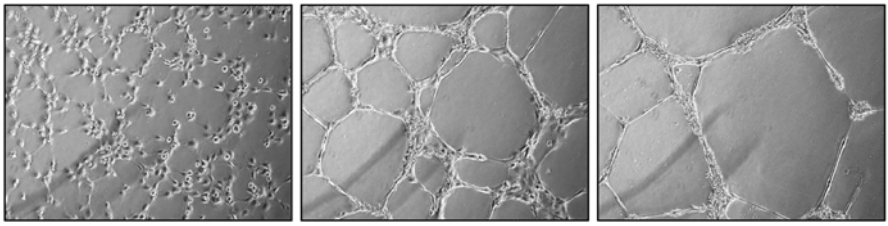

Fig. 4.10 Example of the cells forming tubule like structures captured using Cell-IQ Imagen acquisition software

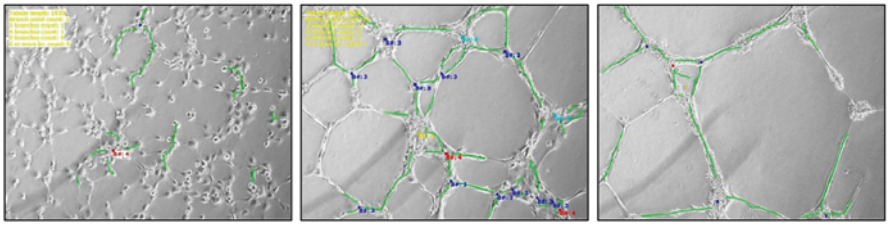

Fig. 4.11 Example of the analysed images using the analyser tubule and branch-point measurement tool

4.5.4 Tubule Formation

As the captured images illustrate, the increased Z-stack of 50 μM ensures that the tubule like structures remain in focus as they form and move in different Z planes over time (Fig. 4.10). As the tubule like structures form the tubule length increases, followed by a small decrease as the tubule network expands forming longer network extensions (Fig. 4.12).

4.6 Troubleshooting

In order to ensure that the software can accurately analyse the closure of the scratch, it is critical that the cells are confluent prior to the scratch being created. In addition tubule formation is reliant on the correct seeding density being applied to the wells.

Careful planning is required to ensure that the necessary data is obtained from live cell imaging experiment. To ensure the images remains in focus the size of the Z-stack must be appropriate for the samples being imaged. The number of regions imaged must also be carefully selected; the addition of too many could result in the time taken to return to the same region to be too long, resulting in key events being missed.

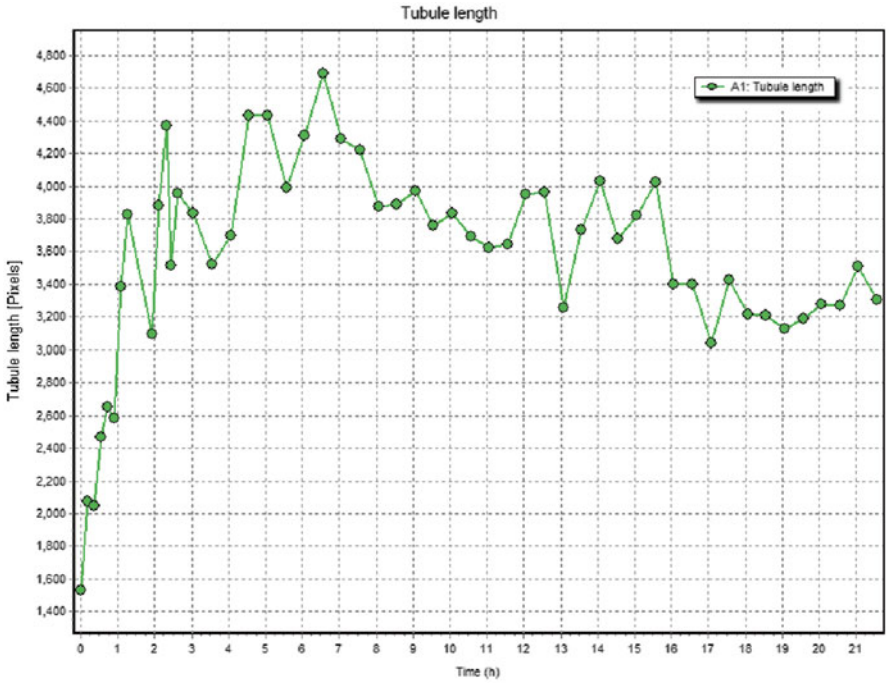

Fig. 4.12 Graphical results illustrating the total tubule length over time as the tube -like structures form in matrigel

If imaging with fluorescence, care must be taken not to damage the cells by imaging with too high an exposure or too frequently.

4.7 Applications and Discussions

Traditionally the assays used to assess in vitro angiogenesis are end point and provide only a snapshot of the biological response. By employing live cell imaging a complete over view of the response can be obtained, which is especially important when investigating the effects of specific factors (pro or anti) on a dynamic processes such as angiogenesis.

Not only does this powerful technique facilitate automated capture and results processing, reducing time and labour costs, it will also confirm the appropriateness of previously chosen time points in former studies. In addition, the ability to collect a series of data points from the same population of cells enables more detailed studies to be performed with fewer samples, and as the imaging process is non-destructive these samples can subsequently undergo further analysis e.g. RNA or protein extractions.

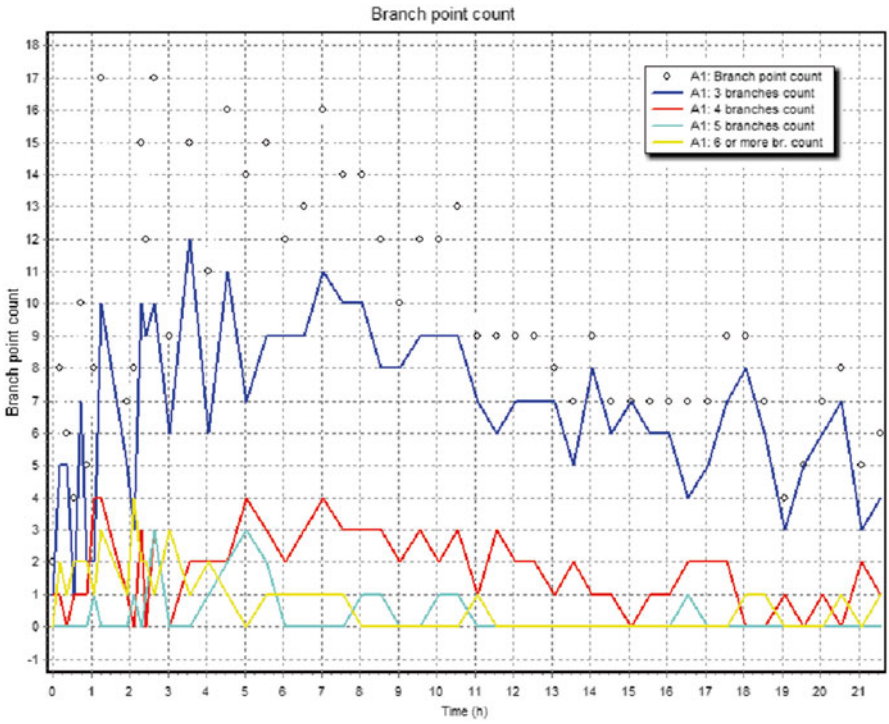

Fig. 4.13 Graphical results illustrating the different branch-point count over time as the tubule like structures form in the matrigel

The use of machine vision to classify and quantify different cell populations provides the user with an intelligent but achievable approach to analysing various experimental data sets, including complex models such as co-culture experiments. The ability to identify different cell types and phases from phase contrast images alone eliminates the need for fluorescent dyes in many experimental protocols. For those experiments where protein expression is of interested and can be determined by a fluorescent signal, the fluorescence image acquisition and analysis tool enables information on specific expression patterns to be obtained.

Initially developed in the seventeenth century, microscopes have since become an integral part of cell biology laboratories. Recent developments have resulted in the availability of live cell imaging platforms, allowing numerous biological processes to be studied in real time.

Although still developing, this informative technique is already enriching the data sets of many studies, demonstrating compatibility with both traditional techniques such as PCR, western blotting and more complex genomic methods such as microarray studies [5].

References

1. Huttunen TT, Sundberg M et al (2011) An automated continuous monitoring system: a useful tool for monitoring neuronal differentiation of human embryonic stem cells. Stem Cell Stud 1(e10):71–77
2. Mikkola M, Toivonen S et al (2013) Lectin from Erythrina cristagalli supports undifferentiated growth and differentiation of human pluripotent stem cells. Stem Cells Dev 22(5):707–716
3. Toivonen S, Ojala M et al (2013) Comparative analysis of targeted differentiation of human induced pluripotent stem cells (hiPSCs) and human embryonic stem cells reveals variability associated with incomplete transgene silencing in retrovirally derived hiPSC lines. Stem Cell Trans. doi: 10.5966/sctm.2012-0047
4. Vuoristo S, Toivonen S et al (2013) A novel feeder-free culture system for human pluripotent stem cell culture and induced pluripotent stem cell derivation. PLoS One 8(10):e76205
5. Kivi N, Greco D et al (2008) Genes involved in cell adhesion, cell motility and mitogenic signalling are altered due to HPV 16 ES protein expression. Oncogene 27:2532–2541
6. Talmana V, Amadiob M et al (2013) The C1 domain-targeted isophthalate derivative HMI-1b11 promotes neurite outgrowth and GAP-43 expression through PKC activation in SH-SY5Y cells. Pharmacol Res 73:44–54
7. Palazzolo G, Horvath P et al (2012) The flavonoid isoquercitrin promotes neurite outgrowth by reducing Rho A activity. PLoS One 7(11):e49979
8. Talman V, Tuominen RK et al (2011) C1 Domain-targeted isophthalate derivatives induce cell elongation and cell cycle arrest in HeLa cells. PLoS One 6(5):e20053. doi:10.1371/journal.pone.0020053
9. Bosutti A, Qui J et al (2013) Targeting p35/cdk5 signalling via CIP-peptides promotes angiogenesis in hypoxia. PLoS One 8(9):e75538
10. Ball SG, Worthington JJ et al (2013) Mesenchymal stromal cells: inhibiting PDGF receptors or depleting fibronectin induces mesodermal progenitors with endothelial potential. Stem Cells 10. doi: 10.1002/stem.1538
11. Sonka M, Hlavac V et al (1999) Image processing, analysis, and machine vision, 2nd edn. PWS Pub, Pacific Grove
12. Tarvainen J, Saarinen M et al (2002) Creating images with high data contents for microworld applications. Ind Sys Rev:17–23
13. Tozer GM, Akerman S et al (2008) Blood vessel maturation and response to vascular-disrupting therapy in single vascular endothelial growth factor-A isoform–producing tumors. Cancer Res 68(7):2301–2311
14. Walter MNM, Wright KT et al (2010) Mesenchymal stem cell-conditioned medium accelerates skin wound healing: an in vitro study of fibroblast and keratinocyte scratch assays. Exp Cell Res 316(7):1271–1281